

# Accepted Manuscript

Long term features of diabetic retinopathy in streptozotocin-induced diabetic Wistar rats

Asieh Naderi, Reza Zahed, Leila Aghajanpour, Fahimeh Asadi Amoli, Alireza Lashay



PII: S0014-4835(18)30812-1

DOI: <https://doi.org/10.1016/j.exer.2019.04.025>

Reference: YEXER 7657

To appear in: *Experimental Eye Research*

Received Date: 5 November 2018

Revised Date: 10 April 2019

Accepted Date: 23 April 2019

Please cite this article as: Naderi, A., Zahed, R., Aghajanpour, L., Amoli, F.A., Lashay, A., Long term features of diabetic retinopathy in streptozotocin-induced diabetic Wistar rats, *Experimental Eye Research* (2019), doi: <https://doi.org/10.1016/j.exer.2019.04.025>.

This is a PDF file of an unedited manuscript that has been accepted for publication. As a service to our customers we are providing this early version of the manuscript. The manuscript will undergo copyediting, typesetting, and review of the resulting proof before it is published in its final form. Please note that during the production process errors may be discovered which could affect the content, and all legal disclaimers that apply to the journal pertain.

**Long Term Features of Diabetic Retinopathy in Streptozotocin-induced Diabetic Wistar Rats**

Asieh Naderi<sup>a</sup>, Reza Zahed<sup>b</sup>, Leila Aghajanpour<sup>c</sup>, Fahimeh Asadi Amoli<sup>d</sup>, Alireza Lashay<sup>a</sup>

<sup>a</sup> Translational Ophthalmology Research Center, Farabi Eye Hospital, Tehran University of Medical Sciences, Tehran, Iran. asiehnaderi@gmail.com

<sup>b</sup> Department of Emergency Medicine, Imam Khomeini Hospital Complex, Faculty of Medicine, Tehran University of Medical Sciences, Tehran, Iran. rzahed@gmail.com

<sup>c</sup> Stem Cell Preparation Unit, Farabi Eye Hospital, Tehran University of Medical Sciences, Tehran, Iran. aghajanpourleila@gmail.com

<sup>d</sup> Department of pathology, Farabi Eye Hospital, Tehran University of Medical Sciences, Tehran, Iran. path1383@yahoo.com

Declarations of interest: none

Corresponding Author: Alireza Lashay

Mailing address: Farabi Eye Hospital, Qazvin Sq, Tehran, Iran. Postal Code: 1336616351.

Tel: +9821-55421080

Fax: +9821-55421010

E-mail: Lashay@tums.ac.ir, Lashay3601@gmail.com

**Abstract**

Diabetic retinopathy is a complication of diabetes and a leading cause of vision loss among working-age adults. To assess whether the Wistar rat with Streptozotocin (STZ)-induced diabetes is a suitable animal model of human proliferative diabetic retinopathy we evaluated the vascular changes to assess the diabetic retinopathy (DR) stages in this model. After two weeks of intraperitoneal STZ (55mg/kg) injection in male Wistar rats (270-300 g), they were considered diabetic with persistent blood glucose levels  $\geq 16.65$  mmol/L. The diabetic and control rats were investigated after 1, 3, 6 and 9 months by electroretinography, Evans blue assay, dextran fluorescence retinal angiography, and retinal histopathological studies. Retinal vascular permeability in the diabetic groups increased significantly in all diabetic groups. The amplitude of a- and b-waves decreased significantly in all diabetic groups compared with the age-matched control groups. The latent time of a-waves in the diabetic groups were delayed at 3 months of diabetes and this delay remained relatively constant till 9 months following the onset of diabetes. Although the latent time of b-wave in the diabetic groups increased slightly, a significant difference was found right at 9 months of diabetes. Vascular density and branching point numbers significantly decreased in the diabetic eyes at 3 and 6 months while they increased at 9 months, which was not significant. Intraretinal hemorrhage and ischemic changes were detected in the half of diabetic rats after 6 months and considered as preproliferative stage of diabetic retinopathy. Although preproliferative changes were detected in all diabetic rats at 9 months, half of them showed vitreous neovascularization attached to retina and retinal folds which can be considered as proliferative stage of DR. Intraretinal hemorrhage, extensive leakage of fluorescein, retinal folds, and vitreous neovascularization were the most prominent findings of severe and proliferative diabetic retinopathy in a fraction of the STZ-induced diabetic rats which were comparable to that of the human patients. STZ-induced diabetic rats can be considered to be a potentially useful model for studies on pathogenesis and treatment of diabetic retinopathy in human.

**Key words:** Animal model; Diabetes; Diabetic retinopathy; Retinal neovascularization; Streptozotocin.

## 1. Introduction

Diabetic retinopathy (DR) is the most common complication of diabetes and one of the major causes of blindness in working-age people worldwide (Cai and McGinnis, 2016). DR, initially was considered as a microvascular complication of diabetes and classified as either nonproliferative (NPDR) or proliferative (PDR) based on the presence of neovascularization (Fong et al., 2004; Gardner et al., 2011). However, there is increasing evidence, that all cells housed in the retina are affected. So, DR is also thought to be a neurodegenerative disease in addition to a microvascular complication (Szabó et al., 2017). The most common manifestations of NPDR include microaneurysms, increased vascular permeability, intraretinal hemorrhages, retinal capillary non-perfusion, and intraretinal microvascular abnormality (IRMA). Proliferative diabetic retinopathy is characterized by neovascularization on the retina and posterior surface of the vitreous and can lead to retinal detachment (Fong et al., 2004; Gardner et al., 2011).

To clarify the complicated nature of the disease, the effects of new drugs or improve existing therapies, studies using diabetic animal models are essential (Kern, 2008). These models can be classified as chemically induced, spontaneous, and genetically created, based on the experimental approaches (Cai and McGinnis, 2016). Chemically-induced streptozotocin (STZ) model is one of the most popular diabetic models and has been routinely used in basic studies and therapeutic drug experiments. This model exhibits rapid onset of hyperglycemia within a few days after STZ injection in rats (Lai and Lo, 2013). Although different and large number of animal models have been used to assess different aspects of ocular changes in diabetes, few models demonstrate features of severe or proliferative diabetic retinopathy. Variation of the retinal lesions is reported among different species and even within the same species, which can be explained by the genetic background and strain differences (Cai and McGinnis, 2016). STZ- induced diabetic rat models exhibit some of the signs of early DR such as thickening of basement membrane (Agrawal et al., 2012), increased vascular permeability (Qaum et al., 2001), loss of pericytes and the development of acellular capillaries (Roy et al., 2011); however, severe ocular complications such as neovascularization and tractional changes in retina is not demonstrated in these models. One of the reasons for these may be the short duration of the studies; STZ- induced DR rat models are typically studied for up to 20 weeks (Olivares et al., 2017).

It seems that spontaneously diabetic Torii (SDT) rat, a nonobese model of type 2 diabetes, is a good model for studying the severe ocular complications and proliferative retinopathy in type 2 diabetes. Ocular complications such as cataract, neovascular glaucoma, tractional retinal detachment, abnormal retinal vasodilatation, severe fluorescein leakage and proliferative retinopathy were demonstrated in SDT rats of both sexes at ages over 60 weeks (Shinohara, 2013). However, based on our best knowledge, there

is no counterpart of SDT in type 1 diabetes. On the other hand, the SDT model is not readily available in all labs. To assess whether the Wistar rat with STZ-induced diabetes is a suitable animal model of human proliferative diabetic retinopathy we evaluated the vascular changes focusing on neovascularization assessed by dextran fluorescence angiography as well as histological changes at different time points.

## 2. Methods

### 2.1. Animals

Male Wistar rats, weighing 270-300 g, (2 Months) were used in this study. Rats were housed one per cage, at standard temperature and humid environment with 12-hour light/dark cycles with chow and water provided ad Libitum. All experimental procedures were approved by the ethics committee of the Translational Ophthalmology Research Center of Tehran University of Medical Sciences. After an 18-hour fast, rats were injected intraperitoneally (i.p.) with a single dose (55mg/kg) of streptozotocin (STZ: Sigma, St Louis, MO, USA) dissolved in 0.1M cold citrate buffer (pH 4.5) to induce hyperglycemia. Nondiabetic control rats received equivalent volume of citrate buffer only. One week later, rats with blood glucose levels  $\geq 16.65$  mmol/L were considered diabetic. To ensure all animals were satisfactorily diabetic, the experiment was not begin until 2 weeks after streptozotocin was administered. We did not use insulin for the diabetic groups. Blood glucose levels were measured again monthly to confirm diabetic status. Body weights, water, and food intake were monitored two times per week. The cages, wood-chipcarpet and drinking water were changed daily to improve hygiene conditions and prevent infection. Electroretinography (ERG) to assess retinal function, Evans blue (EB) assay to evaluate retinal vascular permeability, FITC-dextran perfusion for observing retinal vessels and histology study to identify changes in retina structure were performed in the diabetic and age-matched control groups at 1, 3, 6, and 9 months of diabetes.

### 2.2. Electroretinography

Flash electroretinography was performed by the electrophysiological test unit (Metrovision, France). Before the test, rats were dark-adapted overnight and prepared under dim red light. The animals were then anesthetized with ketamine and xylazine (100/10 mg/kg). Pupils dilated by 1% tropicamide, and the corneal surface was anesthetized with 0.5% tetracaine hydrochloride. In the process of scotopic ERG, the flash light luminance of 15 dB was set for recording Rod-response. Using a recording electrode (Goldring electrode, 4mm, Roland Consult, Brandenburg, Germany), the electrical response of each retina was recorded. The recording electrode was positioned on the corneal surface, the reference electrode was penetrated into the middle forehead, and the ground electrode was placed on the tail. For each recording, a- and b-wave amplitudes, as well as implicit times of responses, were determined by averaging the responses of the eight light stimuli. The amplitude of a-wave was measured from the baseline to the

negative trough, and the amplitude of the b-wave was measured from the trough of the a-wave to the peak of the b-wave. Latency was measured from stimulus onset to the trough of a-wave and peak of b-wave.

### 2.3. Evans Blue Assay

Blood-retinal barrier breakdown (BRBB) was quantified using the Evans blue method as described previously (Xu et al., 2001) with minor modifications. The diabetic and age-matched control groups were anesthetized with ketamine (100 mg/kg; Alfasan, Netherlands) and xylazine (10 mg/kg; Alfasan Netherlands). Additional anesthesia was provided throughout the procedures as needed. Evans blue (45 mg/kg) was injected over 10 seconds through the tail vein. Immediately after EB injection, the rats turned visibly blue, confirming their uptake and distribution of the dye. To ensure the complete circulation of the dye, the rats were kept on a warm pad for 2 hours. Afterward, at 15-minute intervals, 100  $\mu$ l blood was drawn for 2 hours to obtain the time-averaged plasma Evans blue concentration.

After 2 h, the chest cavity was opened, and rats were perfused with citrate buffer (0.05 M, pH 3.5) for 2 minutes via the left ventricle at 37°C to clear the dye from the vessel. Subsequently, both eyes were enucleated and bisected at the equator. Retinae were carefully dissected under an operating microscope and dried at 70°C for 24 h. Evans blue dye conjugated to serum albumin in the retina was extracted by incubating each sample in 130  $\mu$ l formamide (Sigma) for 18 hours at 70°C. The extract was centrifuged at 65,000 rpm, for 60 minutes at 4°C.

The blood samples were centrifuged at 12,000 rpm for 15 minutes, at 4 °C and diluted 1/100 in formamide prior to spectrometric evaluation. To assess the Evans blue concentration, the absorbance of the retinal extract and plasma samples was measured at 620 nm and measured in comparison with a standard curve. BRBB was calculated using the following equation. Results were expressed as microliters plasma  $\times$  gram retina dry wt<sup>-1</sup> h<sup>-1</sup>.

$$\frac{\text{Evans blue } (\mu\text{g})/\text{Retina dry weight (g)}}{\text{Time averaged Evans blue concentration } (\mu\text{g})/\text{Plasma } (\mu\text{l}) \times \text{Circulation time (h)}}$$

### 2.4. FITC-Dextran Perfusion

Quantification of retinal neovascularization in the flat-mounted retinae was performed according to a previous report (D'amato et al., 1993), with some modifications. Briefly, one milliliter of PBS containing 40 mg/ml Fluorescein isothiocyanate-dextran (average mol wt: 2 $\times$ 10<sup>6</sup>; Sigma, St Louis, MO, USA) was perfused through the left ventricle of the anesthetized rats. After 5 minutes, the eyes enucleated and fixed in 4% paraformaldehyde overnight. Following cornea excision, retinae were removed under a dissecting microscope. The retinae were cut radially from the edge to the equator and then flat mounted in Aqua-Poly/Mount (Polysciences, Warrington, PA). The flat mounts were viewed by fluorescent microscope and photographed. Vascular density and total number of junctions of the capillary network

were calculated from five parts of the retina in each eye using the AngioTool image analysis software 10 (Zudaire et al., 2011).

### 2.5. Histological study

Formalin-fixed, paraffin embedded eyes of the diabetic and age-matched control groups were sectioned (5 $\mu$ m), stained with hematoxylin and eosin (H & E) and examined under the light microscope. Six eyes in each group from different rats were examined. Histopathological changes studied included: intraocular neovascularization and hemorrhage, retinal neovascularization and hemorrhage, retinal gliosis, retinal ischemic changes and infarct, nuclear layers' thickness, ganglion cell number and degenerative changes in the lens. Anterior chamber angle (AC) neovascularization was also evaluated. Intraretinal hemorrhage and ischemic changes were considered as preproliferative diabetic retinopathy and new vessel formation either at the disc or elsewhere and vitreous neovascularization attached to the retina, in addition to the other histopathological findings of preproliferative retinopathy were diagnosed as proliferative phase of diabetic retinopathy.

### 2.6. Cataract formation

Lens appearance was assessed and scored at each time point by visual inspection. The scoring system is according to the classification of (Sampath et al., 2011) as follows: 0 = clear lens, 0.2 = spots, 0.5 = cloudy, and 1 = opaque.

### 2.7. Statistics

The data are presented as means  $\pm$  SD. Two-tailed Student's t-test was used to analyze differences between the diabetic and age-matched control groups at different time points. Two-way analysis of variance (ANOVA) was applied to determine the main effect of group (control, diabetic) and time (duration of diabetes) and their interaction on all parameters using IBM SPSS, version 24 (IBM Corp).  $P < 0.05$  were considered as statistically significant.

## 3. Results

### 3.1. Glycemia and body weight

Rats with a blood glucose concentration higher than 16.65 mmol/L were considered diabetic. The incidence of diabetes induced by a single dose of STZ was 87.5%. Mortality after 3 months was 8.6% and after 6 and 9 months were 16.6%.

Table 1 shows the body weight, food and water intake and blood glucose levels for the diabetic rats and their age-matched control groups. The diabetic rats showed a significant reduced weight in all time points, despite the significant increase in water and food intake compared with the age-matched controls. Furthermore, blood glucose levels were significantly higher in the diabetic groups compared with age-matched control groups. Measuring blood glucose levels monthly showed no change in diabetic status compared with the first post-induction of diabetes; that is, all diabetic animals remained diabetic.

### 3.2. Effects of hyperglycemia on visual function

Figure 1 shows representative ERG recordings under scotopic conditions of the diabetic and control rats. Sustained hyperglycemia led to a significant decrease in the a- and b-wave amplitudes in the early stages. As shown in table 2, the amplitude of the a-wave decreased gradually from 31% at 1 month of diabetes to 53% in 9 months of diabetes. The extent of amplitude reduction was much more significant in b-wave than a-wave in early stages of DR. The b-wave amplitudes of the diabetic groups decreased approximately to 50% in all diabetic groups compared with the age-matched control groups. The latent time of a-wave in the diabetic groups were delayed approximately up to 15% at 3 months of diabetes and this delay remained relatively constant till 9 months following the onset of diabetes. Although the latent time of b-wave in the diabetic groups increased slightly compared with the age-matched control groups; however, significant differences was found right at 9 months of diabetes. In spite of a slight decrease in the amplitude of a- and b-waves at the 9 months in the control group compared with the baseline, there were no significant differences in retinal function during the 9 months follow up. There was a significant main effect of the group on all ERG parameters, a-wave amplitude: ( $F = 227.9, P < 0.001$ ); b-wave amplitude: ( $F = 126.7, P < 0.001$ ); a-wave implicit time: ( $F = 30.3, P < 0.001$ ); b-wave implicit time: ( $F = 6.5, P = 0.013$ ). The effect of time was significant on a-wave amplitude, ( $F = 8, p < 0.001$ ). There was a nonsignificant interaction between these main effects.

### 3.3. Effects of hyperglycemia on blood retinal barrier breakdown

The STZ diabetic rats mimic certain early changes of human DR, including blood-retinal barrier breakdown. Retinal vascular permeability as indicated by EB dye accumulation increased significantly as early as 1 month after the onset of diabetes, with a 2.1-fold elevation over the control level. The hyperpermeability remained at higher levels during the entire experimental period in the diabetic groups, with 2.3, 2.7 and 3.2-fold elevation over the age-matched control groups, at 3, 6, and 9 months of diabetes, respectively, Fig. 2. There was a significant main effect of the group on the retinal vascular permeability ( $F = 112.3, P < 0.001$ ). The main effect of time and the interaction between these main effects were not statistically significant.

### 3.4. Effects of hyperglycemia on vascular changes

To assess retinal neovascularization and vascular leakage we performed dextran fluorescence retinal angiography in the diabetic and age-matched control groups. Five to six eyes from 5-6 rats were assessed in each group. Increased fluorescein leakage, indicative of increased vascular permeability, was observed in the diabetic eyes. Diabetes of 3 months' duration showed increased vascular permeability in limited areas, while examination of retinal flat mounts showed pronounced vascular leakage around optic disk (Fig. 3D) and peripheral retinae (red arrows in Fig. 3E) at 6 and 9 months of diabetes. Four eyes from 6 diabetic eyes showed vascular abnormalities at 9 months of diabetes. Retinal vascular tortuosity

and loop formation (Fig. 3F) were observed at 2 out of the 6 eyes. New vessels formation visualized in diabetic eyes (Fig. 3E, H) at 6 (1 out of the 6 eyes) and 9 months (4 out of the 6 eyes) of diabetes compared with age-matched control groups. Limited non-perfusion areas in peripheral retina detected in 2 out of 6 eyes at 9 months of diabetes (Fig. 3I). No abnormalities were observed in the vascular structure in the age-matched control eyes. Using AngioTool software, vascular density and branching point density were quantified in all diabetic and age-matched control eyes. Vascular density is defined as the percentage of area occupied by vessels inside the explant area and branching point density is defined as the number of vessel junctions normalized per unit area (Zudaire et al., 2011). A statistically significant decrease in vascular density and branching point numbers demonstrated in the diabetic eyes at 3 and 6 months of diabetes compared with the age-matched control group (Fig. 4). Although vascular density and branching point numbers increased in the diabetic group after 9 months, it was not significantly different from that of the control group. There were significant effects of group ( $F = 4.05$ ,  $P = 0.04$ ) and time ( $F = 5.7$ ,  $P < 0.001$ ), as well as a significant interaction between these main effects ( $F = 7.31$ ,  $P < 0.001$ ) on vascular density. There was no significant effect of time ( $F = 20.2$ ,  $P = 0.09$ ), but there was a significant effect of group ( $F = 23.3$ ,  $P < 0.001$ ) on branching point density. The interaction between these effects was significant ( $F = 7.7$ ,  $P < 0.001$ ).

### 3.5. Effects of hyperglycemia on histological change

No histopathological changes were detected on H&E-stained sections in the control eyes at any age (Fig. 5A). Eye sections from the diabetic rats at 1 and 3 months of diabetes except cataract revealed no significant histopathological findings in light microscopic evaluation (Fig. 5B). Mild cataracts started at 1 month of diabetes in some diabetic rat and worsened with the duration of hyperglycemia, as all diabetic rats had matured cataract at 6 and 9 months of diabetes (Fig. 6B). While no cataract formation was detected in the control groups (Fig. 6A).

Half of the eye specimens at 6 months of diabetes showed preproliferative stage of diabetic retinopathy. These changes included retinal and intraocular hemorrhage, AC angle and intraretinal neovascularization, mild focal retinal infarct and retinal gliosis of internal plexiform layer. There were no evidence of ganglion cell loss, internal and external nuclear layer thickness changes, and evidence of proliferative diabetic retinopathy at this duration of diabetes. All eye specimens at 9 months of diabetes showed histopathological findings consistent with preproliferative and proliferative diabetic retinopathy. These finding included retinal and intraocular hemorrhage, retinal ischemic changes and infarct, angle neovascularization, vitreous neovascularization attached to the retina, retinal gliosis, mild ganglion cell loss and decreased inner nuclear layer thickness.

Areas of retinal folds (Fig. 5C) were observed in half of the cases at 9 months of diabetes. At this duration of diabetes, proliferative vascular membrane in vitreous originated from the optic disk and

vitreoretinal traction (Fig. 5F, I) were observed in some cases. Also, massive hemorrhages in the anterior chamber angle (Fig. 5H) of the eye and optic disk (Fig. 5I) were observed in some cases. Collectively, all data indicate that pathology consistent with severe DR or PDR is related to the duration of hyperglycemia.

### 3.6. Effects of hyperglycemia on cataract formation

By visual inspection, cataract formation in diabetic animals detected after 3 months. After 3 months, 9.5% of the lenses of the diabetic rats showed score 0.2, 28.5% showed score 0.5 and 62% showed score 1. After 6 months 9% of the lenses of the diabetic rats showed score 0.5, and 91% showed score 1. All of the diabetic rats after 9 months showed score 1. The lenses in all control groups appeared to be clear and normal.

## 4. Discussion

Diabetic retinopathy is a consequence of diabetes with many structural and functional abnormalities implicated in its development (Mishra et al., 2018). STZ-induced diabetic model is an animal model of human type 1 diabetes and one of the most commonly used models for many aspects of research in diabetes mellitus (Olivares et al., 2017).

In the present study, STZ-treated male Wistar rats exhibited high serum glucose level at one week after STZ injection, and by one month they developed body weight loss, polydipsia, and polyphagia. They also developed cataract by 3 months after diabetes development, which was demonstrated also in the previous studies after 3 months (Agardh et al., 2000; Wang et al., 2015). Blood-retinal barrier breakdown and reduced visual function were found in early stages of DR. The BRBB that occurs in DR is responsible for lots of the vision loss due to diabetes (Díaz-Lezama et al., 2016; Tzeng et al., 2015); the resulting leakage of serum proteins and other blood components into the retina and posterior vitreous can produce loss of light by absorption and/or scattering of light before being sensed by retina (Díaz-Lezama et al., 2016) (Daley et al., 1987). Opacities of the ocular media and cataracts formation in the early stages of diabetes in STZ-induced diabetic rats could affect both amplitudes and implicit times of ERG waves as reported in the cataractous eyes in human (Yamauchi et al., 2016). We did not detect any significant histopathological and vascular findings in light and fluorescein-dextran microscopy in this stage.

Preproliferative stage of diabetic retinopathy was detected in half of the diabetic rats after 6 months. Some of the 9-month diabetic rats developed retinal hemorrhage, retinal folds mimicking tractional retinal changes, venous dilatation, tortuosity and vascular loop formation corresponding to the intraretinal microvascular abnormality (IRMA) seen in human DR; they also showed proliferative vascular membrane in the vitreous body. However, in contrast to humans with diabetic retinopathy, the STZ-induced diabetic rats did not develop microaneurysms in the retina. Vessel density and branching point numbers changed with progression from early to late stages of diabetes as quantified by AngioTool

software. The vessel density and branching point numbers decreased significantly in early stages of diabetes and increased again in late stages of diabetes in the diabetic groups. This oscillatory pattern of vascular density is also evident in human studies, which can be attributed to the dynamic balance among several angiogenic inhibitors and stimulators during the progression of DR (Parsons-Wingerter et al., 2010). Dextran fluorescence angiography showed a cord-like structure in limited areas from mid-peripheral retina mimicking non-perfusion capillary in human.

Although numerous diabetic animal models have shown significant diabetic retinal microvascular lesions, none had DR that closely exhibited the features of human disease (Yamada et al., 2005). Previous studies in STZ-induced diabetic rats reported only early stages of DR (Gong et al., 2013; Zhang et al., 2008), somehow it may be attributed to the short period of diabetes that these models have been studied compared with diabetic patients. There are just a few studies on STZ-induced diabetic rats for a long time that reported severe ocular complications. In 1990, Robinson et al. reported pericyte "ghosts" like those defined in human diabetes approximately 6 to 8 months following STZ-treatment in diabetic rats. Also, they observed capillary dilation, endothelial cell proliferation, and varicose loop formation in some diabetic rats (Robinson et al., 1991). Retinal microaneurysms in trypsin-digested flat mounts of STZ-induced diabetic rats were reported after 100 weeks in 2000 by Su et al (Su et al., 2000). In 2010 Kern et al. compared retinopathy in three strains of diabetic rats, they reported degeneration of retinal capillaries and pericyte ghosts in Lewis and Wistar rats compared to nondiabetic controls after 8 months. In contrast, these changes were not significant in Sprague Dawley rats at the same duration of diabetes (Kern et al., 2010). In this study, some severe diabetic ocular complications were demonstrated in long time follow up. It seems that duration of diabetes is a strong predictor for onset and progression of retinopathy (Fong et al., 2004). Considering entire life span, every-day life of a laboratory rat resembles a human month, so a diabetic rat with 9 months (270 day) diabetes mimics a human with 22 years diabetic duration (Sengupta, 2013).

In human, DR is a prototypical microvascular disorder associated with microaneurysms, intraretinal hemorrhages, capillary non-perfusion, intraretinal microvascular abnormalities, and neovascularization (Gardner et al., 2011) on its progressive stages. However, in rodents, these stages were not completely identical with human and it seems that some of the early diabetic retinal changes observed in diabetic patients bypassed in the STZ- induced diabetic rats that has been reported in SDT rat previously (Kakehashi et al., 2006).

## 5. Conclusion

This study detected abnormalities in visual function and vascular leakage in the STZ-induced diabetic rats after a short time. We showed that the severe retinal changes could be detected in STZ-induced diabetic rat in a long time duration of diabetes. Some changes including vitreous

neovascularization attached to the retina and vitreoretinal traction are very similar to the changes that occur in human proliferative diabetic retinopathy. Tractional changes may have been due to pre-retinal membrane formation that exerts tractional forces on the retina and pulls it away from the layer underneath. Neovascularization demonstrated after 9 months in this study can be a proof for the development of proliferative retinopathy in the STZ-induced male Wistar rats which can be a potential target model for studying the pathogenesis and new treatments of DR.

### **Acknowledgement**

This work was supported by the Tehran University of Medical Sciences (grant number: 32108).

### **Declarations of interest**

None.

### **Author contribution**

AN contributed to conception and design, acquisition of data and interpretation of data, and drafted the article. AN and LA performed the animal experiments and the ex vivo experiments. RZ contributed to analysis of data and critically revised the manuscript. FAA performed the histological examinations and interpreted the histological data. AL contributed to the interpretation of data, supervised the manuscript preparation, and critically revised the manuscript. All authors read the manuscript and approved the final version to be published.

### **References**

- Agardh, E., Hultberg, B., Agardh, C.-D., 2000. Effects of inhibition of glycation and oxidative stress on the development of cataract and retinal vessel abnormalities in diabetic rats. *Curr. Eye Res.* 21, 543-549.
- Agrawal, S.S., Naqvi, S., Gupta, S.K., Srivastava, S., 2012. Prevention and management of diabetic retinopathy in STZ diabetic rats by *Tinospora cordifolia* and its molecular mechanisms. *Food Chem. Toxicol.* 50, 3126-3132.
- Cai, X., McGinnis, J.F., 2016. Diabetic retinopathy: animal models, therapies, and perspectives. *Journal of diabetes research* 2016.
- D'amato, R., Wesolowski, E., Smith, L.H., 1993. Microscopic visualization of the retina by angiography with high-molecular-weight fluorescein-labeled dextrans in the mouse. *Microvasc. Res.* 46, 135-142.
- Daley, M.L., Watzke, R.C., Riddle, M.C., 1987. Early loss of blue-sensitive color vision in patients with type I diabetes. *Diabetes Care* 10, 777-781.
- Díaz-Lezama, N., Wu, Z., Adán-Castro, E., Arnold, E., Vázquez-Membrillo, M., Arredondo-Zamarripa, D., Ledesma-Colunga, M.G., Moreno-Carranza, B., De La Escalera, G.M., Colosi, P., 2016. Diabetes enhances the efficacy of AAV2 vectors in the retina: therapeutic effect of AAV2 encoding vasoinhibin and soluble VEGF receptor 1. *Lab. Invest.* 96, 283-295.
- Fong, D.S., Aiello, L., Gardner, T.W., King, G.L., Blankenship, G., Cavallerano, J.D., Ferris, F.L., Klein, R., 2004. Retinopathy in diabetes. *Diabetes Care* 27, s84-s87.
- Gardner, T.W., Abcouwer, S.F., Barber, A.J., Jackson, G.R., 2011. An integrated approach to diabetic retinopathy research. *Arch. Ophthalmol.* 129, 230-235.
- Gong, C.-Y., Lu, B., Hu, Q.-W., Ji, L.-L., 2013. Streptozotocin induced diabetic retinopathy in rat and the expression of vascular endothelial growth factor and its receptor. *Int J Ophthalmol* 6, 573-577.

- Kakehashi, A., Saito, Y., Mori, K., Sugi, N., Ono, R., Yamagami, H., Shinohara, M., Tamemoto, H., Ishikawa, S.e., Kawakami, M., 2006. Characteristics of diabetic retinopathy in SDT rats. *Diabetes Metab. Res. Rev.* 22, 455-461.
- Kern, T., Miller, C., Tang, J., Du, Y., Ball, S., Berti-Matera, L., 2010. Comparison of three strains of diabetic rats with respect to the rate at which retinopathy and tactile allodynia develop. *Mol. Vis.* 16, 1629-1639.
- Kern, T.S., 2008. *Animal Models of Diabetic Retinopathy, Retinal and Choroidal Angiogenesis*. Springer, pp. 81-102.
- Lai, A.K.W., Lo, A.C., 2013. Animal models of diabetic retinopathy: summary and comparison. *Journal of diabetes research* 2013.
- Mishra, M., Duraisamy, A.J., Kowluru, R.A., 2018. Sirt1-A Guardian of the Development of Diabetic Retinopathy. *Diabetes* 67, 745-754.
- Olivares, A.M., Althoff, K., Chen, G.F., Wu, S., Morrisson, M.A., DeAngelis, M.M., Haider, N., 2017. Animal models of diabetic retinopathy. *Curr. Diab. Rep.* 17, 93-109.
- Parsons-Wingerter, P., Radhakrishnan, K., Vickerman, M.B., Kaiser, P.K., 2010. Oscillation of angiogenesis with vascular dropout in diabetic retinopathy by VESSEL GENERATION analysis (VESGEN). *Invest. Ophthalmol. Vis. Sci.* 51, 498-507.
- Qaum, T., Xu, Q., Jousseaume, A.M., Clemens, M.W., Qin, W., Miyamoto, K., Hasselmann, H., Wiegand, S.J., Rudge, J., Yancopoulos, G.D., 2001. VEGF-initiated blood-retinal barrier breakdown in early diabetes. *Invest. Ophthalmol. Vis. Sci.* 42, 2408-2413.
- Robinson, W.G., McCaleb, M.L., Feld, L.G., Michaelis, O.E., Mercandetti, M., 1991. Degenerated intramural pericytes ('ghost cells') in the retinal capillaries of diabetic rats. *Curr. Eye Res.* 10, 339-350.
- Roy, S., Nasser, S., Yee, M., Graves, D.T., Roy, S., 2011. A long-term siRNA strategy regulates fibronectin overexpression and improves vascular lesions in retinas of diabetic rats. *Mol. Vis.* 17, 3166-3174.
- Sampath, S., McLean, L.A., Buono, C., Moulin, P., Wolf, A., Chibout, S.-D., Pognan, F., Busch, S., Shangari, N., Cruz, E., 2011. The use of rat lens explant cultures to study the mechanism of drug-induced cataractogenesis. *Toxicol. Sci.* 126, 128-139.
- Sengupta, P., 2013. The laboratory rat: relating its age with human's. *Int. J. Prev. Med.* 4, 624-630.
- Shinohara, M., 2013. The spontaneously diabetic torii rat: an animal model of nonobese type 2 diabetes with severe diabetic complications. *Exp. Diabetes Res.* 2013.
- Su, E.-N., Alder, V., Yu, D.-Y., Cringle, S., Yogesan, K., 2000. Continued progression of retinopathy despite spontaneous recovery to normoglycemia in a long-term study of streptozotocin-induced diabetes in rats. *Graefes Arch. Clin. Exp. Ophthalmol.* 238, 163-173.
- Szabó, K., Énzöly, A., Dékány, B., Szabó, A., Hajdú, R.I., Radovits, T., Mátyás, C., Oláh, A., Laurik, L.K., Somfai, G.M., 2017. Histological evaluation of diabetic neurodegeneration in the retina of Zucker diabetic fatty (ZDF) rats. *Sci. Rep.* 7, s1598-s2017.
- Tzeng, T.-F., Hong, T.-Y., Tzeng, Y.-C., Liou, S.-S., Liu, I.-M., 2015. Consumption of polyphenol-rich Zingiber Zerumbet rhizome extracts protects against the breakdown of the blood-retinal barrier and retinal inflammation induced by diabetes. *Nutrients* 7, 7821-7841.
- Wang, H.-M., Li, G.-X., Zheng, H.-S., Wu, X.-Z., 2015. Protective effect of resveratrol on lens epithelial cell apoptosis in diabetic cataract rat. *Asian Pac. J. Trop. Med.* 8, 153-156.
- Xu, Q., Qaum, T., Adamis, A.P., 2001. Sensitive blood-retinal barrier breakdown quantitation using Evans blue. *Invest. Ophthalmol. Vis. Sci.* 42, 789-794.
- Yamada, H., Yamada, E., Higuchi, A., Matsumura, M., 2005. Retinal neovascularisation without ischaemia in the spontaneously diabetic Torii rat. *Diabetologia* 48, 1663-1668.
- Yamauchi, Y., Mochizuki, J.-i., Hirakata, A., Uda, S., 2016. Single flash electroretinograms of mature cataractous and fellow eyes. *Clin. Ophthalmol.* 10, 2031-2034.

Zhang, J., Wu, Y., Jin, Y., Ji, F., Sinclair, S.H., Luo, Y., Xu, G., Lu, L., Dai, W., Yanoff, M., 2008. Intravitreal injection of erythropoietin protects both retinal vascular and neuronal cells in early diabetes. *Invest. Ophthalmol. Vis. Sci.* 49, 732-742.

Zudaire, E., Gambardella, L., Kurcz, C., Vermeren, S., 2011. A computational tool for quantitative analysis of vascular networks. *PLoS One* 6, e27385.

### Figure legends

**Fig. 1.** Control and diabetic ERG responses measured in dark-adapted state. The flash light luminance of 15 dB was set for recording. Each recording was determined by averaging the responses of the eight light stimuli. Red lines show the peak of a- and b-waves in the control, while the black arrows indicate the peak of a- and b-waves in the diabetic rats.

**Fig. 2.** Quantitative analysis of the Evans blue leakage. The retinal permeation of Evans blue-stained albumin was evaluated at 1, 3, 6, and 9-month time points in the diabetic and age-matched control groups. Data are means  $\pm$  SD, (n = 10-12 eyes from 5-6 rats/group)

**Fig. 3.** Fluorescence micrographs of fluorescein-dextran perfused retinæ in flat-mount preparation. Low and high-magnification fluorescein angiographs of retinal whole mounts obtained from control (A, B, C) and diabetic (D, E, F) rats 9 months post-STZ injection, (n = 5-6 eyes from 5-6 rats/group). The uniform retinal vascular distribution was visible in all control eyes. No vascular abnormalities were observed in the control eyes, while areas of retinal neovascularization and extensive fluorescein leakage around the optic disk, and tortuous vessels (D) were visible at 9 months of diabetes. (E) The pattern of increased vascular permeation and neovascularization were seen in the mid-peripheral retina flat-mount at 6 and 9 months of diabetes (red arrows). Higher magnification fluorescein angiographs of the mid-peripheral retinæ from a 9-month control (C) and diabetic (F) rat. Significant vascular dilation, vascular loops formation and shunting (red arrows) were observed in diabetic retinæ. (H) Increased vascular density and collateral vessel formation in a diabetic retina compared with (G) age-match control retina. (I) Non-perfusion area in mid-peripheral retina from a 9-month diabetic rat (white square) with capillary non-perfusion (red arrow). Scale bar: 100  $\mu$ m.

**Fig. 4.** AngioTool was used to evaluate the vascular density and branch points in each eye. Representative retinæ from a control (A) and diabetic rats at 3 (B), 6 (C), and 9 (D) months and the resulting images after analysis of the retinæ in the control and diabetic rats. (E and F) Graphical representation of the analysis performed on 5-6 individual retinæ in each group. Data are means  $\pm$  SD. Scale bar: 200  $\mu$ m.

**Fig. 5.** Histology of retina specimens from the control and diabetic rats. (n = 6 eyes from 6 rats/group). (A) H&E staining of retina from the control rats showing no abnormalities at 1, 3, 6 and 9-month time points. (B) H&E staining of retina from the diabetic rats showing no abnormalities at 1 and 3 months of

diabetes, while vascular hemorrhage (yellow arrows) were visible in diabetic eyes at 6 and 9 months of diabetes. Low (C) and high-magnification (D) photographs obtained from 9-month diabetic rats showing intraretinal hemorrhage and eosinophilic necrotic material in the inner layer of the retina. (E) Intraocular neovascularization on inner surface of the retina and vitreous cavity may indicate that proliferative retinopathy is developing. Yellow arrows show new blood vessels on the inner surface of the retina. The formation of several retinal folds can be seen in this sections. Low (F) and high-magnification (G) photographs obtained from 9-month diabetic rats showing hemorrhage and proliferative vascular membrane in vitreous. Massive hemorrhage and neovascularization were visible in anterior angle (H) and optic nerve head (I). Scale bar: 50  $\mu$ m.

**Fig. 6.** Photographic illustration of eyes and representative histopathology lens images (400X) in control (A) and diabetic (B) rats taken after 9 months. In the control animals, the eye section showed normal lens without degeneration of background substance and lens fibers. The Cataractous lenses of the STZ-treated rats revealed degenerative and destructive changes.

**Table 1** Average weight, water and food intake and blood glucose levels of the control and diabetic groups at 1, 3, 6 and 9-month time points

Groups	1-month		3-month		6-month		9-month	
	Control	Diabetic	Control	Diabetic	Control	Diabetic	Control	Diabetic
<b>Weight (g)</b>	328±22	282±22*	360±15	285±24*	383±26	290±25*	405±26	300±22*
<b>Water (ml/day)</b>	50±10	215±22*	48±4	214±29*	52±8	209±23*	51±8	207±16*
<b>Food (g/day)</b>	19±4	31±5*	24±3	39±4*	22±3	39±3*	22±3	40±3*
<b>Glucose (mmol/L)</b>	5.8±0.6	25.2±3.1*	5.9±0.5	26.1±3.0*	6.2±0.9	27±3.2*	6.1±0.7	27.4±3.4*

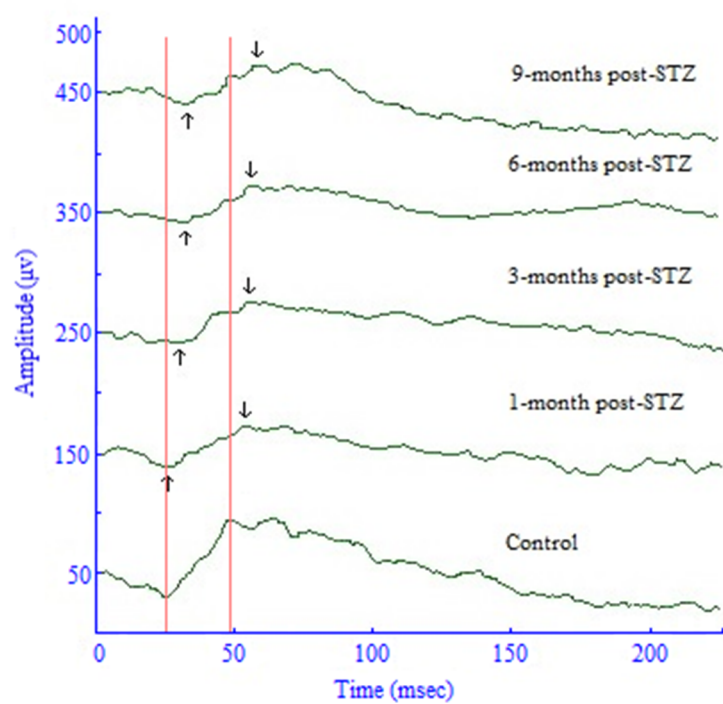
Data are mean ± SD. \* different from control p < .001, n= 10-12 rats/group.

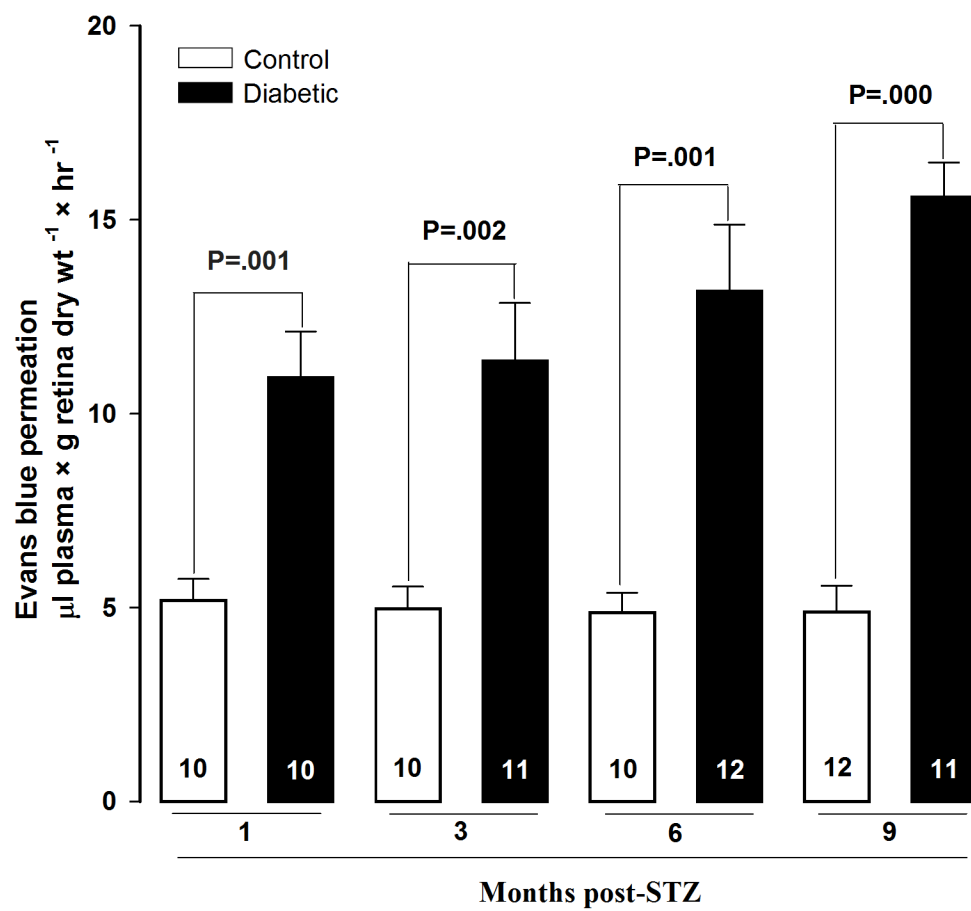
**Table 2** The amplitude and latent time of rod responses from the control and diabetic rats at 1, 3, 6 and 9-month time points

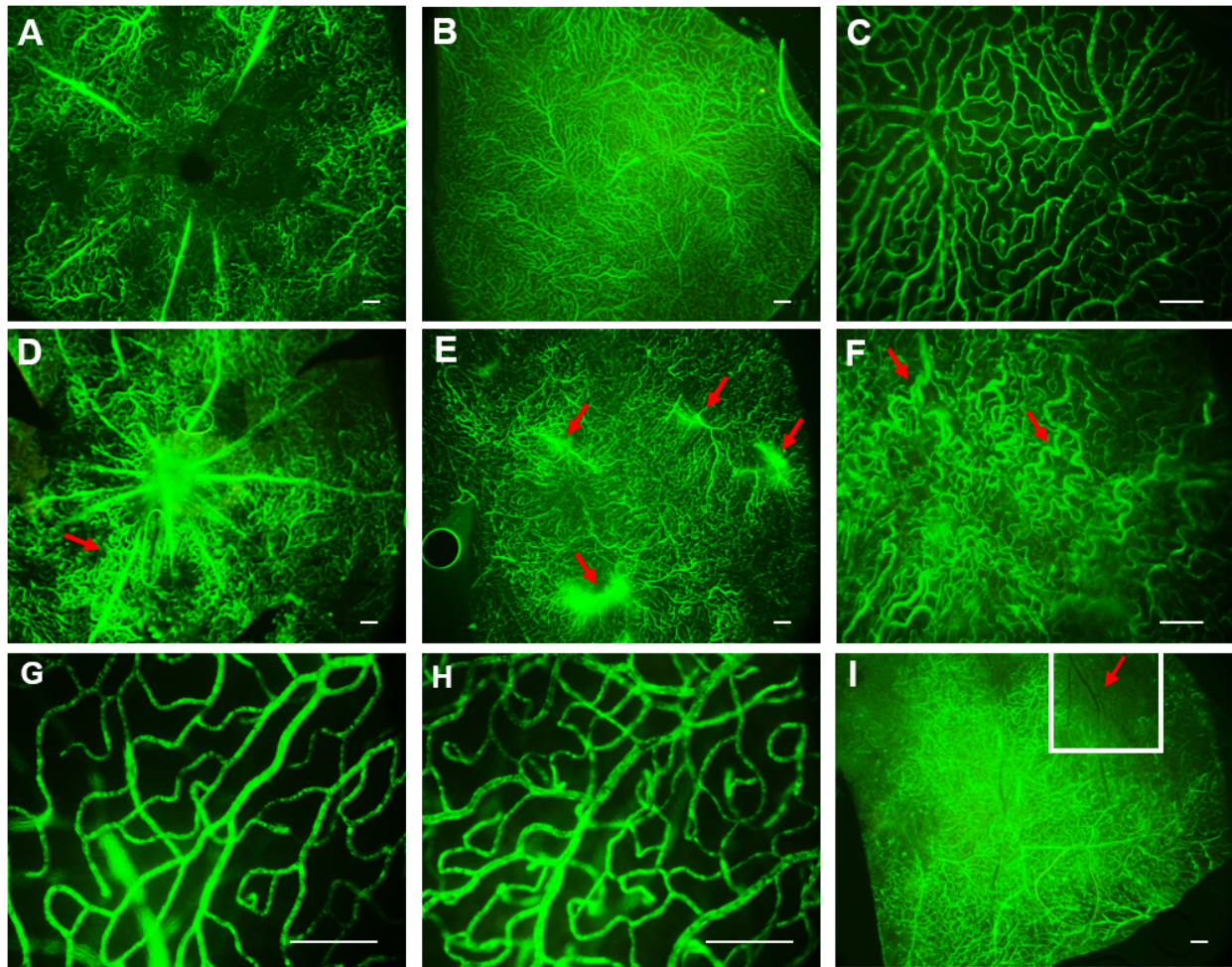
Groups	Baseline	1-month		3-month		6-month		9-month	
		Control	Diabetic	Control	Diabetic	Control	Diabetic	Control	Diabetic
<b>a-wave</b>									
<b>Amplitude (µV)</b>	19.63 ± 4.41	18.71 ± 2.50	12.94 ± 2.63**	18.09 ± 2.55	9.88 ± 2.29**	17.05 ± 2.49	8.91 ± 1.95**	17.09 ± 3.52	7.96 ± 1.97**
<b>Latent Time (ms)</b>	22.21 ± 2.31	23.28 ± 1.79	23.58 ± 2.96	22.45 ± 1.83	25.91 ± 3.20*	22.05 ± 2.54	27.16 ± 3.98**	22.49 ± 2.24	26.88 ± 4.16*
<b>b-wave</b>									
<b>Amplitude (µV)</b>	62.35 ± 16.26	60.69 ± 13.69	30.54 ± 8.79**	63.17 ± 17.71	32.94±10.73**	55.81 ± 15.47	28.32 ± 6.68**	52.07 ± 12.31	26.20 ± 9.75**
<b>Latent Time (ms)</b>	49.11 ± 6.72	50.08 ± 5.33	50.63 ± 6.52	51.72 ± 4.07	53.65 ± 7.73	52.01 ± 8.44	56.25 ± 5.66	51.77 ± 5.96	58.50 ± 7.04*

Data are means ± SD. \* different from control p < .05, \*\*different from control p < .001, n= 18-20 eyes/group.

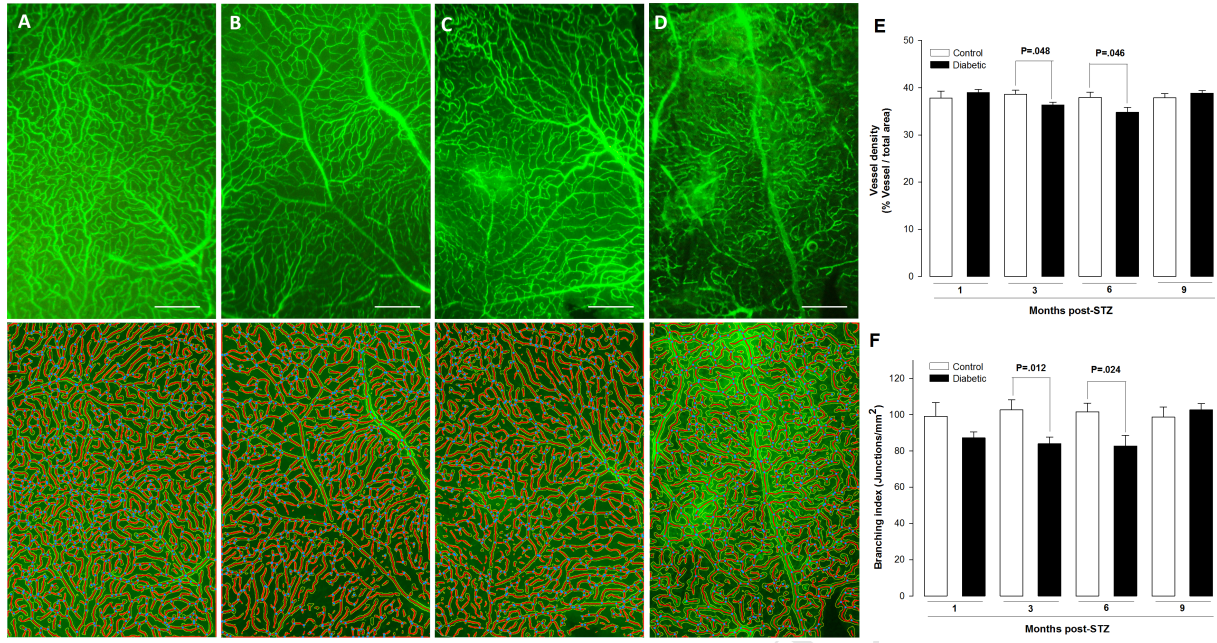
ACCEPTED MANUSCRIPT

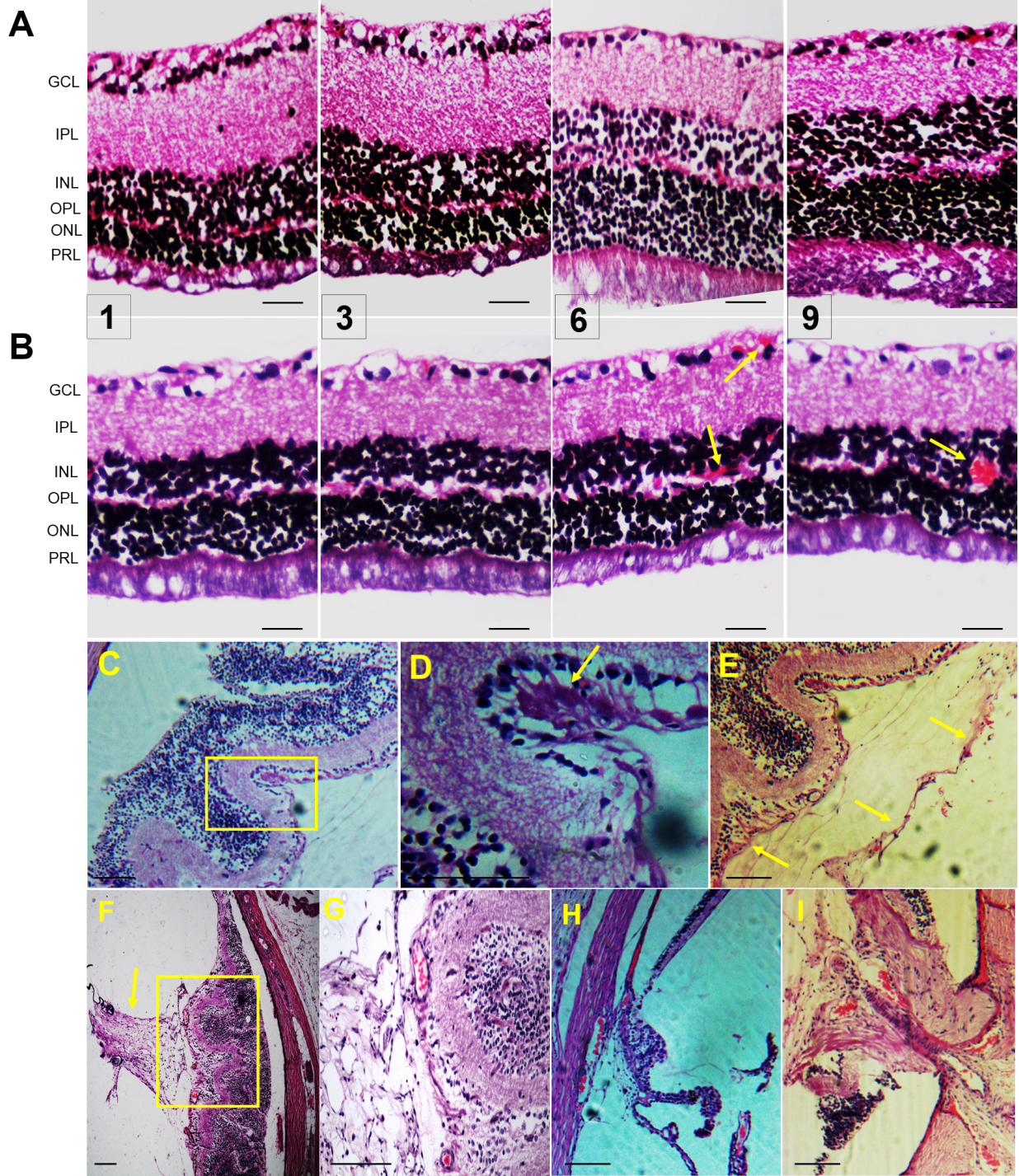


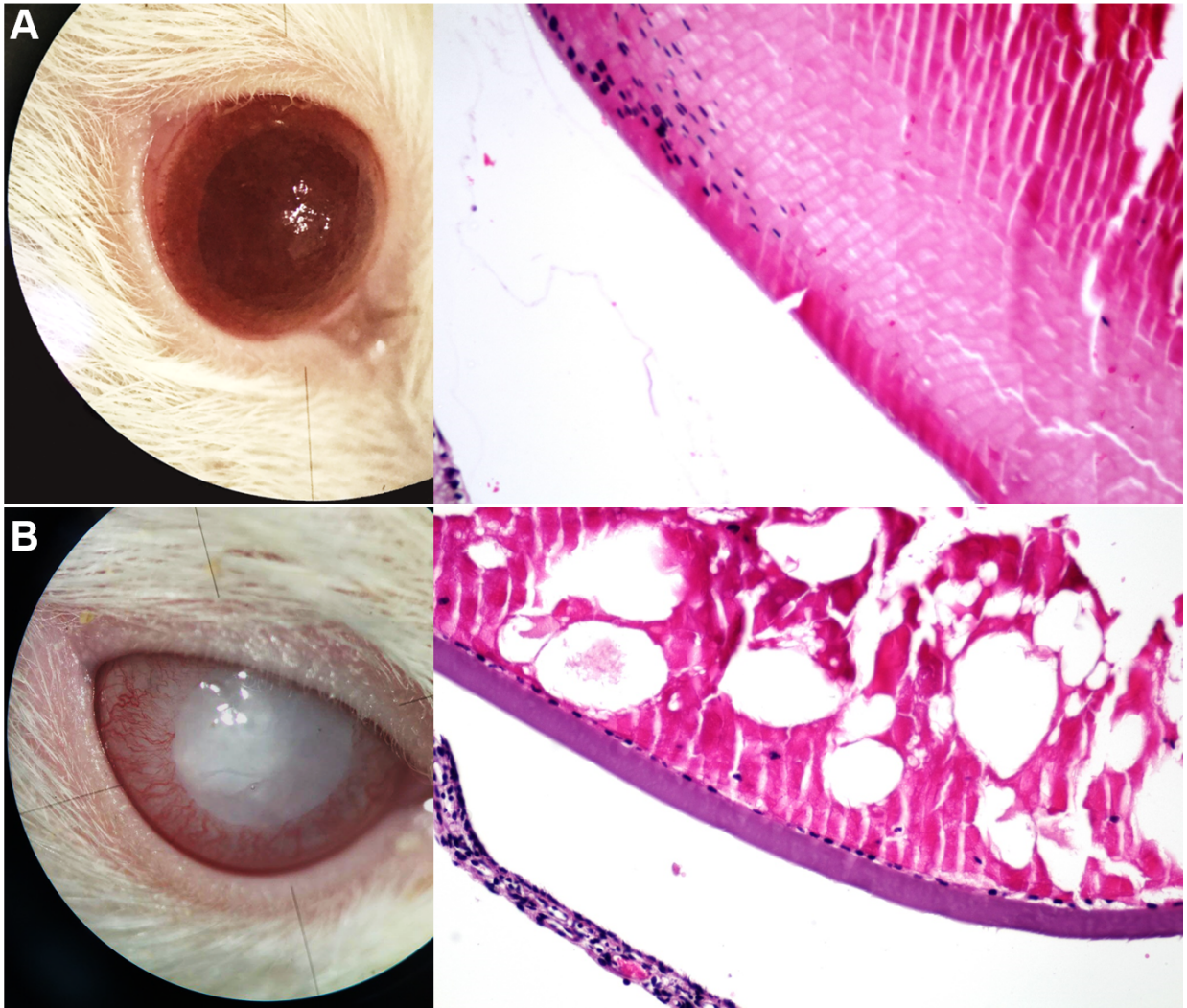




ACCEPTED







ACCEPTED

**Highlights:**

- Severe DR needs a long term follow up to be discovered in STZ-induced diabetic rats
- Retinal folding and vitreous neovascularization were the most prominent findings
- STZ-induced diabetes is a suitable model in resource-limited settings for DR assessment